2-1-2005

Structure of the p115RhoGEF rgRGS domain-Galpha13/i1 chimera complex suggests convergent evolution of a GTPase activator

Zhe Chen
Department of Biochemistry, The University of Texas Southwestern Medical Center, 5323 Harry Hines Boulevard, Dallas, Texas 75390, USA.

William D. Singer

Paul C. Sternweis

Stephen R. Sprang
stephen.sprang@umontana.edu

nature structural & molecular biology

Structure of the p115RhoGEF rgRGS domain–Gα13/i1 chimera complex suggests convergent evolution of a GTPase activator

Zhe Chen[1], William D Singer[2], Paul C Sternweis[2] & Stephen R Sprang[1,3]

p115RhoGEF, a guanine nucleotide exchange factor (GEF) for Rho GTPase, is also a GTPase-activating protein (GAP) for G12 and G13 heterotrimeric Gα subunits. The GAP function of p115RhoGEF resides within the N-terminal region of p115RhoGEF (the rgRGS domain), which includes a module that is structurally similar to RGS (regulators of G-protein signaling) domains. We present here the crystal structure of the rgRGS domain of p115RhoGEF in complex with a chimera of Gα13 and Gαi1. Two distinct surfaces of rgRGS interact with Gα. The N-terminal βN–αN hairpin of rgRGS, rather than its RGS module, forms intimate contacts with the catalytic site of Gα. The interface between the RGS module of rgRGS and Gα is similar to that of a Gα–effector complex, suggesting a role for the rgRGS domain in the stimulation of the GEF activity of p115RhoGEF by Gα13.

The GEF for Rho, p115RhoGEF[1,2], is a potential regulatory link between G protein–coupled receptors that activate the G12 class of heterotrimeric G proteins and their effectors in Rho-mediated pathways that lead to cytokinesis and transformation[3–5]. The C-terminal half of p115RhoGEF contains tandemly arranged DH and PH domains typical of RhoGEFs[6]. The N terminus contains a GAP domain with remote sequence similarity to the RGS family of protein domains[1,7]. p115RhoGEF shows specific GAP activity toward Gα13 and Gα12 (ref. 1), and binding to Gα13 stimulates its GEF activity[2]. This exchange factor is therefore capable of acting as both a negative regulator and a downstream effector of Gα13.

RGS domains have divergent amino acid sequences[7,8] but share a conserved α-helical fold (the 'RGS box') of ~120 residues[9]. Biochemical[10–13] and crystallographic[9,14] studies of these domains show that they preferentially form complexes with Gα subunits bound to GDP-Mg^{2+}-AlF_4^-, a transition-state analog of GTP hydrolysis. RGS domains seem to promote GTPase activity by stabilizing catalytic conformations of the switch I and switch II regions[9,14] and of the conserved catalytic arginine and glutamine residues within these structures (Arg200 and Gln226 in Gα13). The RGS regions of p115RhoGEF[1] and its homologs, LARG, Lsc, PDZRhoGEF and GTRAP48 (refs. 15–18), differ from the canonical RGS domains. The RGS boxes of the RhoGEFs have <15% amino acid sequence identity with those in other RGS subtypes. In contrast to other RGS-containing proteins, p115RhoGEF requires two elements outside of the conserved RGS box[19] for binding to Gα and GAP activity. These include the EDEDFE sequence within the 42-residue segment that precedes the RGS box[20] and the C-terminal extension of ~70 residues beyond the RGS box, which is required for expression as a soluble protein domain[19]. In p115RhoGEF[21] and PDZRhoGEF[22], this C-terminal extension folds into a layer of helices that packs against the core of the RGS box via hydrophobic interactions. In this study, the N-terminal fragment of p115RhoGEF (residues 1–239) required for full GAP activity is referred to as the rgRGS domain. Mutagenic analysis[20] suggests that the binding surface formed between the RGS box of rgRGS with Gα13 differs in molecular detail from that observed in complexes of RGS4 with Gαi1, or of RGS9 with transducin (Gαt). In particular, the crucial asparagine (residue 128 in RGS4) that orients the catalytic glutamine of Gα substrates is a proline (residue 113) in rgRGS. Mutation of this proline does not greatly affect the GAP activity of the rgRGS domain or its ability to bind Gα13 (ref. 20).

Gα13, which can be produced only with very low yield in insect cells[23], is refractory to expression in bacteria. To overcome this limitation, we engineered a chimera of Gα13 and Gαi1 (Gα13/i1) that is overexpressed in bacteria and functions as Gα13. We determined the three-dimensional structure of a stable complex between this Gα13/Gαi1 chimera and the rgRGS domain of p115RhoGEF. The structure of the complex suggests a novel G protein GAP mechanism that is mediated by the N-terminal structural elements outside of the RGS box, which form extensive contacts with the helical domain and the switch regions of the Gα subunit. The interface between the RGS box of rgRGS and Gα also shares similarity with those observed in structures of Gα–effector complexes. This structure thus provides new insights into GTPase acceleration by RGS proteins, the specificity of rgRGS domains toward G12 class Gα subunits, and activation of p115RhoGEF by Gα13. Our results also suggest that GAP function may have been acquired independently in different branches of the homologous RGS superfamily.

[1]Department of Biochemistry, [2]Department of Pharmacology and [3]The Howard Hughes Medical Institute, The University of Texas Southwestern Medical Center, 5323 Harry Hines Boulevard, Dallas, Texas 75390, USA. Correspondence should be addressed to S.R.S. (stephen.sprang@utsouthwestern.edu).

Published online 16 January 2005; doi:10.1038/nsmb888

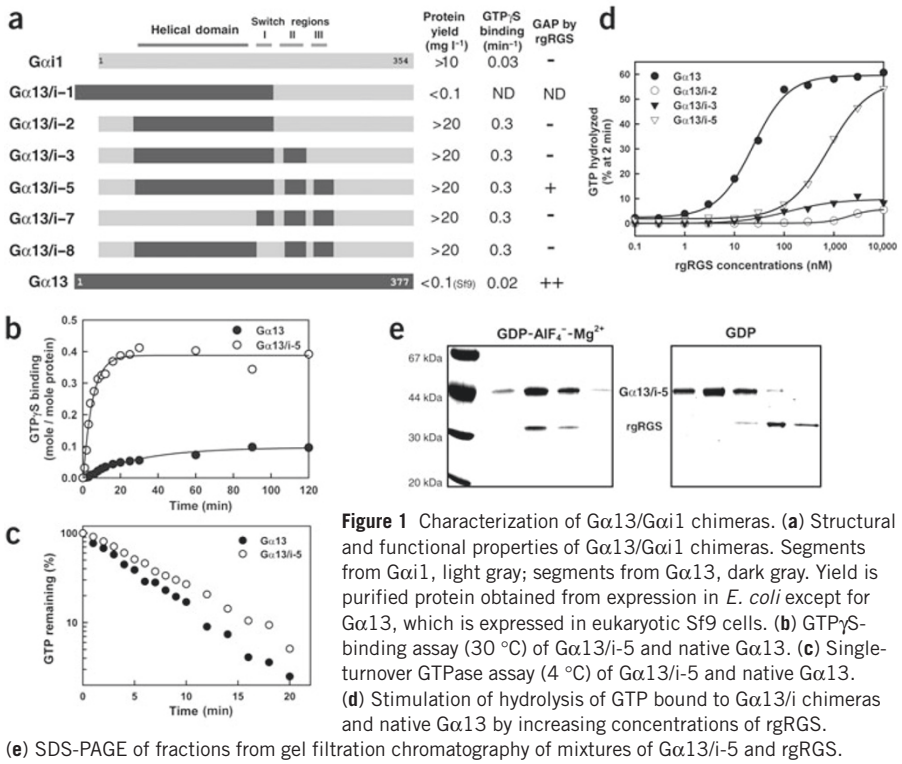

Figure 1 Characterization of Gα13/Gαi1 chimeras. (**a**) Structural and functional properties of Gα13/Gαi1 chimeras. Segments from Gαi1, light gray; segments from Gα13, dark gray. Yield is purified protein obtained from expression in *E. coli* except for Gα13, which is expressed in eukaryotic Sf9 cells. (**b**) GTPγS-binding assay (30 °C) of Gα13/i-5 and native Gα13. (**c**) Single-turnover GTPase assay (4 °C) of Gα13/i-5 and native Gα13. (**d**) Stimulation of hydrolysis of GTP bound to Gα13/i chimeras and native Gα13 by increasing concentrations of rgRGS. (**e**) SDS-PAGE of fractions from gel filtration chromatography of mixtures of Gα13/i-5 and rgRGS. Gα13/i-5 and rgRGS form a stable complex in the presence of GDP-AlF_4^--Mg^{2+} (left), but not with GDP alone (right).

RESULTS

Characterization of Gα13/Gαi1 chimeras

The rgRGS domain of p115RhoGEF can be readily produced in bacteria and retains full GAP activity[24]. In contrast, Gα13 is refractory to expression in bacteria. However, Gαi1, which has 39% sequence identity with Gα13, can be efficiently overexpressed as a functional protein in *Escherichia coli*. Encouraged by similar experiments with other Gα proteins[25,26], we generated a series of chimeras of Gα13 and Gαi1 (Gα13/i1 chimeras) with the goal of obtaining molecules that are efficiently expressed as soluble proteins in *E. coli* but have functional properties characteristic of Gα13, in particular the ability to interact functionally and specifically with the rgRGS domain of p115RhoGEF. As observed by characterization of several constructs (**Fig. 1a**), this was accomplished with Gα13/i-5, a chimera based on Gαi1 but containing the three switch regions and the helical domain of Gα13. Gα13/i-5 binds guanine nucleotides (**Fig. 1b**), hydrolyzes GTP (**Fig. 1c**) and is a substrate of rgRGS (**Fig. 1d**). The chimera is not a substrate for RGS4, which recognizes Gαi1 (data not shown). Dissociation of GDP is more rapid from Gα13/i-5 than from Gα13 or Gαi1. Evidently, Gα13/i-5 and the other chimeric proteins have lower affinity for GDP and presumably for GTP. Nevertheless, the intrinsic GTPase activity of Gα13/i-5 is similar to that of Gα13. Although rgRGS is less potent (5%) as a GAP for Gα13/i-5 than for Gα13, it seems to be similarly efficacious in stimulating the same extent of GTP hydrolysis in both substrates (**Fig. 1d**). Gα13/i-7, which contains the switch regions but not the helical domain of Gα13, is not a substrate of rgRGS (**Fig. 1a**). Gα13/i-5 forms a stable complex with the rgRGS domain in the presence of GDP, Mg^{2+} and AlF_4^-, but not with GDP alone (**Fig. 1e**). The dissociation constant (K_d) for binding of Gα13/i-5 with the rgRGS domain of p115RhoGEF is 3–5 μM in the presence of GDP, Mg^{2+} and AlF_4^- as determined by isothermal titration calorimetry; the K_d increases by at least an order of magnitude in the presence of GTPγS and Mg^{2+}. In addition, Gα13/i-5 with an activating mutation (Q226L) stimulates Rho-dependent transcription in cultured cells (data not shown).

Structure determination of the complex

The rgRGS–Gα13/i-5 complex was formed by mixing a molar excess of rgRGS with Gα13/i-5 activated with GDP, Mg^{2+} and AlF_4^-. The three-dimensional structure of the rgRGS–Gα13/i-5 complex (**Fig. 2**) was determined at a resolution of 2.8 Å. The final atomic model comprises residues 46–371 of Gα13/i-5, residues 16–37, 44–86, 93–122 and 133–233 of the p115RhoGEF rgRGS domain, GDP, AlF_4^-, Mg^{2+} and 84 water molecules. The remaining residues of Gα13/i-5 and the rgRGS domain are disordered.

The asymmetric unit of the crystal contains two rgRGS–Gα13/i-5 complexes related by a two-fold axis of rotation (**Fig. 2b**). The dimer interface buries ~3,600 $Å^2$ of solvent-accessible surface area and is stabilized by the following interactions: first, between the βN strand of the dyad-related molecule (designated 2) and βN–αN of the reference molecule (designated 1 in **Fig. 2b**); second, between the α2, α8 helices of rgRGS (1) and the αA2, αB helices of Gα13/i-5 (2); and last, between the loops connecting the αG and α4 helices of the two adjacent Gα13/i-5 molecules. Whereas these structural data suggest a potential role for dimerization in function, dimer formation is not evident from gel filtration chromatography of the rgRGS–Gα13/i-5 complex. Members of the p115RhoGEF family have been reported to oligomerize, but through their C-terminal domains[27,28].

Structure of Gα13/i-5

Gα13/i-5, like all other Gα subunits, consists of a Ras-like domain and an α-helical domain that is unique to the heterotrimeric G proteins. The Ras-like domain of Gα13/i-5 (residues 15–77 and 198–376) differs from that of Gαi1 by 17 amino acid substitutions, mostly in switches I and III (**Fig. 2c**), and the structures of the two domains are essentially identical; the r.m.s. deviation of corresponding Cα atoms is 0.5 Å. The active site of Gα13/i-5 shows strong electron density for GDP, AlF_4^-, Mg^{2+} and an axial water molecule bound to AlF_4^-. The structure of the catalytic site, together with the arrangement of GDP-Mg^{2+}-AlF_4^-, is similar to that in the corresponding RGS4–Gαi1 complex[9]. No distortion of the nucleotide-binding mode relative to the latter complex is evident that would explain the increased dissociation rate of nucleotide from the active site of Gα13/i-5. The helical domain of Gα13 differs from that of Gαi1 by 81 amino acid substitutions (**Fig. 2c**), and the structures of these domains (residues 78–197 in Gα13/i-5) superimpose with an r.m.s. deviation of 1 Å (see **Supplementary Fig. 1** online). A notable feature of the helical domain of Gα13 that is not present in other known Gα structures is the helix-turn-helix element (the 'helical insert') preceding αC (**Fig. 2a**,**c**). Hydrogen bonds between Gln134 and Gly135 of this element and Arg201 (substituted by valine or asparagines in other Gα proteins, see **Supplementary Table 1** online) tether switch I to the helical insert (see below). Helix αB of Gα13 is shifted toward its N terminus by a full helical turn. Helix αC of Gα13 is shortened by a full helical turn at its N terminus. The two long helices of the helical

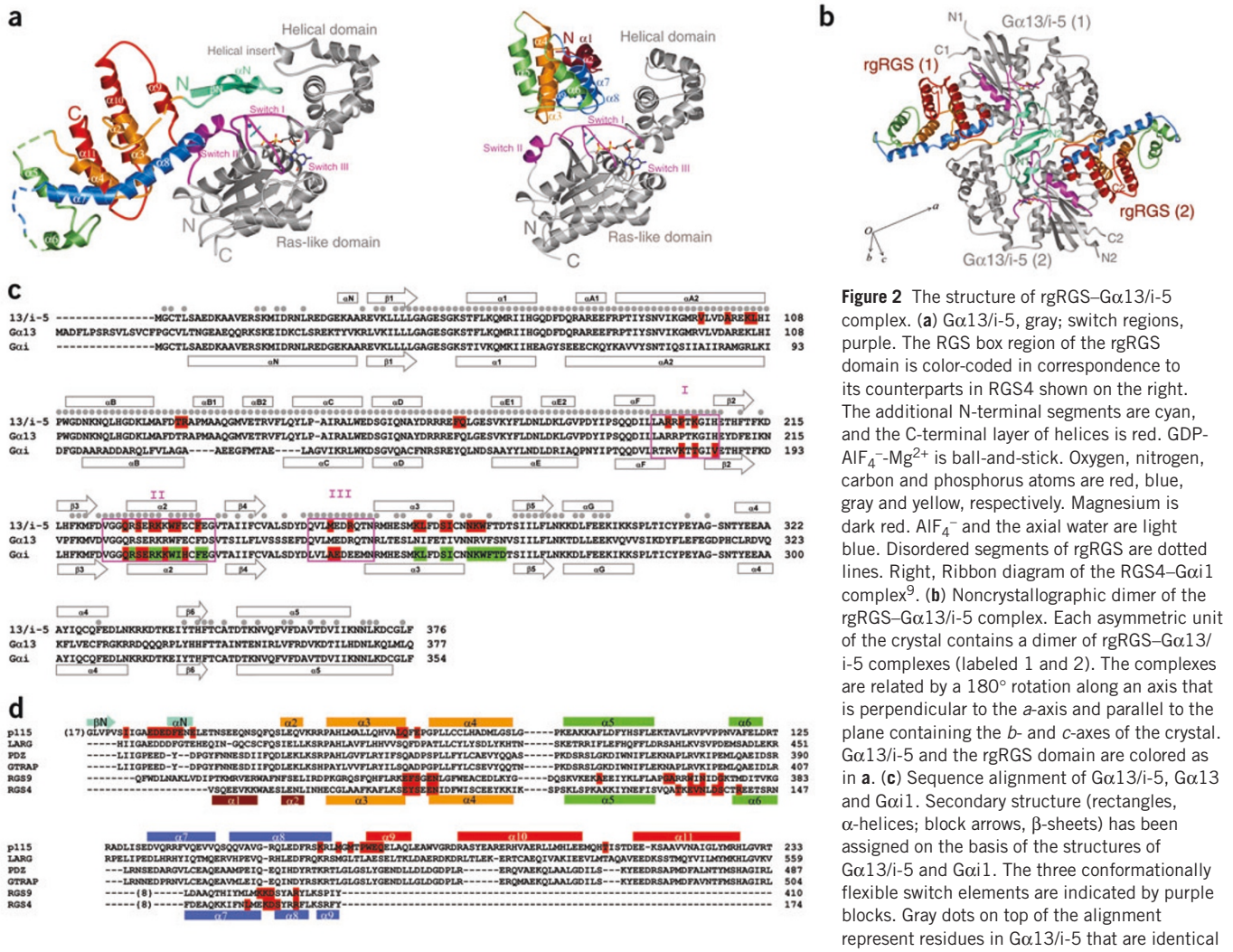

Figure 2 The structure of rgRGS–Gα13/i-5 complex. (**a**) Gα13/i-5, gray; switch regions, purple. The RGS box region of the rgRGS domain is color-coded in correspondence to its counterparts in RGS4 shown on the right. The additional N-terminal segments are cyan, and the C-terminal layer of helices is red. GDP-AlF_4^--Mg^{2+} is ball-and-stick. Oxygen, nitrogen, carbon and phosphorus atoms are red, blue, gray and yellow, respectively. Magnesium is dark red. AlF_4^- and the axial water are light blue. Disordered segments of rgRGS are dotted lines. Right, Ribbon diagram of the RGS4–Gαi1 complex[9]. (**b**) Noncrystallographic dimer of the rgRGS–Gα13/i-5 complex. Each asymmetric unit of the crystal contains a dimer of rgRGS–Gα13/i-5 complexes (labeled 1 and 2). The complexes are related by a 180° rotation along an axis that is perpendicular to the *a*-axis and parallel to the plane containing the *b*- and *c*-axes of the crystal. Gα13/i-5 and the rgRGS domain are colored as in **a**. (**c**) Sequence alignment of Gα13/i-5, Gα13 and Gαi1. Secondary structure (rectangles, α-helices; block arrows, β-sheets) has been assigned on the basis of the structures of Gα13/i-5 and Gαi1. The three conformationally flexible switch elements are indicated by purple blocks. Gray dots on top of the alignment represent residues in Gα13/i-5 that are identical to corresponding residues in Gα13. Residues contacting rgRGS in Gα13/i-5 and RGS4 in Gαi1 are red. Residues in Gαs or Gαt that contact effectors are green. (**d**) The amino acid sequences of rgRGS domains were aligned with two members of the RGS family for which crystal structures have been determined. Colored bars represent helices with color codes that match the ribbon diagrams in **a** (for rgRGS) or in **b** (for RGS4). Residues in rgRGS, RGS4 or RGS9 that are involved in contacts with Gα13/i-5, Gαi1 or Gαt, respectively, are red.

domain, αA and αE in Gαi1, are each broken into two shorter helices, αA1-αA2 and αE1-αE2, respectively, in Gα13.

The rgRGS–Gα13/i-5 interface

The interface between Gα13/i-5 and rgRGS buries a solvent-accessible surface area of 2,900 Å^2 and comprises two distinct regions of contact. The first involves the N-terminal β-turn-α subdomain of rgRGS (residues 17–39: βN–αN, **Fig. 2a**), which is inserted in the trough between the helical domain and switches I–III of Gα13/i-5. The second contact surface is formed by the RGS subdomain of rgRGS (residues 44–233: α2–α11), which packs against switch II and the α3 helix of Gα13/i-5. The Gα-binding surface of rgRGS is predominantly negatively charged (**Fig. 3**) and complements the positively charged binding surface of Gα13/i-5. A subset of residues that contribute to this binding surface, mostly lysines and arginines from the helical domain and the switch regions, are unique to the G12 class of Gα subunits. In contrast, the Gα-binding surfaces of RGS4 (ref. 9) and RGS9 (ref. 14) are predominantly positively charged and complement the negatively charged surfaces of Gαi1 and Gαt, respectively.

Interaction between βN–αN of rgRGS and Gα13/i-5

The N-terminal βN–αN hairpin of rgRGS, rather than its RGS subdomain, forms the closest contacts with the catalytic site of Gα13/i-5 (**Fig. 4a**,**b**) and buries ~1,600 Å^2 of solvent-accessible surface. The negatively charged sequence Glu27–Glu32 anchors the interaction and probably mediates the GAP activity of the rgRGS domain. An earlier study has shown that rgRGS constructs bearing the E27K or F31A mutations cannot bind to Gα13 and have no GAP activity; mutations at other positions in this sequence also cause severe defects[20]. Accordingly, rgRGS with point mutations at Glu27 stimulated the GTPase activity of Gα13 with potencies that parallel the decreasing conservation of side chain charge and volume at the mutation site (Glu > Asp > Ala > Lys; **Fig. 4c**).

The mechanism of rgRGS GAP activity may be analogous to that used by RGS4, RGS9 and their homologs, but it is achieved by structural elements in the N terminus rather than the RGS box (**Fig. 4d**). Interactions that may be important to GAP activity include the salt bridge between the catalytic Arg200 in switch I of Gα13/i-5 with Glu27 of rgRGS. The catalytic arginine is believed to contact the γ-phosphate and β-γ bridge

oxygen atoms during GTP hydrolysis[29,30]. Direct stabilization of this switch I arginine by residues from RGS domains has not been reported in other structures of RGS–Gα complexes. Phe31 in rgRGS seems to be the functional analog of Asn128 in RGS4. In contrast, Pro113 in rgRGS, the structural cognate of Asn128, is remote from the surface of Gα13/i-5. The aromatic side chain of Phe31 is flanked by side chains of Pro202 and Lys204 of switch I and Met257 of switch III in Gα13/i-5, and is in van der Waals contact with the conserved catalytic Gln226 in switch II. Phe31 may serve to orient the backbone carbonyl moiety of Thr203 that binds the nucleophilic water during GTP hydrolysis, and orient the side chain of Gln226 to facilitate its hydrogen bond to the same nucleophilic water. GTRAP48 or PDZRhoGEF, which binds to Gα13 but has little or no GAP activity[18,19], has an αN segment that seems to be shorter than that of p115RhoGEF (**Fig. 2d**). Spatial mismatch of the N-terminal acidic cluster and the bulky residue following it, with respect to its binding site on Gα13, may account for the reduced GAP activity of GTRAP48 or PDZRhoGEF.

Switch III plays a more prominent role in the interaction of Gα13/i-5 with rgRGS than is evident in the RGS complexes of Gαi1 and Gαt[9,14]. The switch III Arg260 forms an ion-pair with Asp28 from rgRGS and a hydrogen bond with the main chain carbonyl oxygen of Ile23. Met257 from switch III is in close proximity to Phe31 from rgRGS. Gα13/i-3, in which switch III residues are derived from Gαi1, fails to interact with the rgRGS domain of p115RhoGEF (**Fig. 1a**,**d**). The helical insert also contributes to the rgRGS–Gα13/i-5 interface via ion pair interactions between Arg128 of Gα and Glu29 and Glu32 of rgRGS. In the structures of RGS4–Gαi1 and RGS9–Gαt, the helical domains are involved in few contacts with the RGS domains. A summary of protein-protein contacts is given in **Supplementary Table 2** online.

The N-terminal βN–αN segment of the rgRGS domain is both necessary and sufficient for the GAP activity of p115RhoGEF. A peptide corresponding to residues 14–34 of p115RhoGEF had GAP activity toward Gα13 and Gα13/i-5 (**Fig. 4e**,**f**) but not toward Gαi1 (see **Supplementary Fig. 2** online). An F31A mutation in the same peptide abolished its GAP activity toward Gα13 or Gα13/i-5. A shorter peptide (residues 22–34) missing βN also had GAP activity. However, the potency of these peptides was ≤1,000-fold that of the rgRGS domain, suggesting that the RGS subdomain provides substantial stabilization of the complex.

Interaction between the RGS subdomain of rgRGS and Gα13/i-5

The RGS subdomain of rgRGS, which includes the RGS box, packs against the surface of switch II that is distal to the catalytic site of Gα13/i-5 (**Fig. 5a**), and thus seems to bolster the interaction of switch II with αN of rgRGS. The α3–α4, α8–α9 and α10–α11 loops and helix α8 of rgRGS are all involved in contacts with Gα13/i-5 (**Fig. 2d**). The α10–α11 loop is present only in the rgRGS family of RGS domains[21,22]. Like αN, the Gα-proximal surface of the RGS subdomain of rgRGS is negatively charged (**Fig. 3**) and packs predominantly against switch II, the α3 helix and the α3–β5 loop of Gα13/i-5, which are positively charged. This latter interface buries ~1,300 Å^2 of solvent-accessible surface. The α8–α9 loop (residues 162–168) from rgRGS lies at the center of the interface and packs against switch II of Gα13/i-5. The side chains of Met165 and Pro167 from rgRGS project into a hydrophobic pocket surrounded by residues from switch II and the α3 helix (**Fig. 5a**). The α8–α9 loop moves closer to switch II (farther from the core of the rgRGS domain) upon binding to Gα13/i-5. The latter hydrophobic contacts are complemented by ion pairs and hydrogen-bonding interactions, several of which take advantage of structural features that are specific to the Gα12 family (**Figs. 2c** and **5a**; see **Supplementary Table 2** online). Mutations of Gln69, Glu71 or Lys160 of rgRGS reduce binding to Gα13 and GAP activity[20], but these losses are not as severe as those resulting from mutation of residues in αN.

The interface between the RGS subdomain of rgRGS and switch II–α3 of Gα13/i-5 mimics features of effector-Gα interfaces between Gαs and the catalytic domains of adenylyl cyclase (AC)[31] and between Gαt and the γ subunit of cGMP phosphodiesterase (PDEγ)[14]. In all three complexes, a bulky, hydrophobic side chain from the effector (Met165 in rgRGS, Phe991 in the C2 domain of AC and Trp70 in PDEγ) projects into the hydrophobic cleft between switch II and the α3 helix of Gα (**Fig. 5b**). The switch II and α3 residues involved in the interaction are largely conserved or similar in Gα proteins (**Figs. 2c** and **5b**). However, several of the rgRGS-contacting residues in the α3–β5 loop of Gα13/i-5, which is derived from Gαi1 (**Fig. 2c**), are substituted by different residues in Gα13. In particular, residue 280 at the C terminus of α3 is a tryptophan in Gα13/i-5, but a valine or leucine in the G12 class Gα subunits. In the rgRGS–Gα13/i-5 complex, and in the two effector–Gα complexes (**Fig. 5b**), this residue or its cognate docks into a hydrophobic pocket of the Gα binding partner. However, replacement of all the residues of

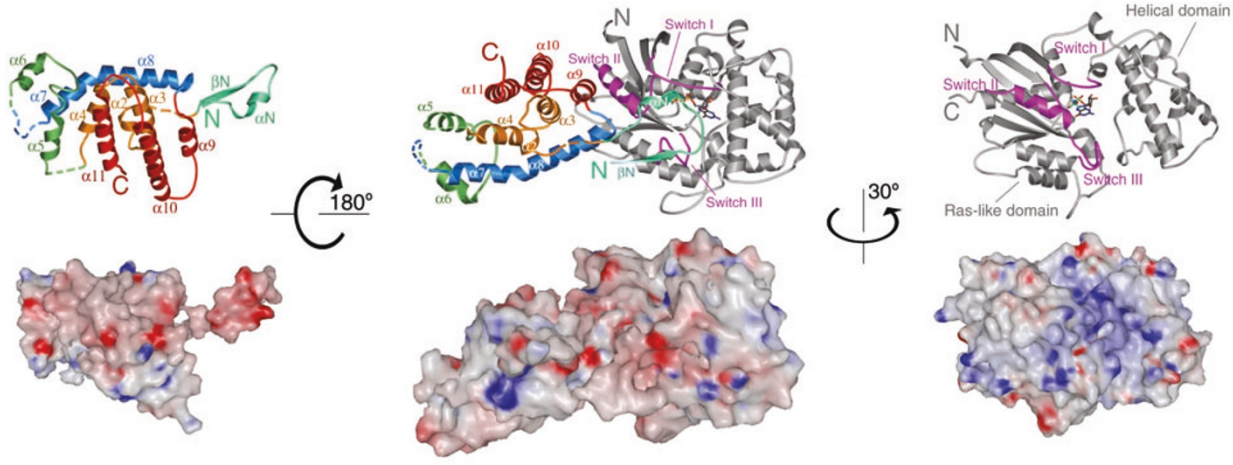

Figure 3 Electrostatic potentials of the rgRGS–Gα13/i-5 complex. Ribbon diagrams depicting the tertiary structures (top row, same coloring scheme as in **Fig. 2a**) and the corresponding solvent-accessible surfaces (bottom row) of the rgRGS domain (left), the complex (center) and Gα13/i-5 (right). Solvent-accessible surfaces are colored according to electrostatic potential in the range of –10 kT (red) to +10 kT (blue), where k is the Boltzmann's constant and T is temperature (K). The complex is rotated 90° about the horizontal with respect to the view shown in **Figure 2a**. The rgRGS domain and Gα13/i-5 are rotated as indicated.

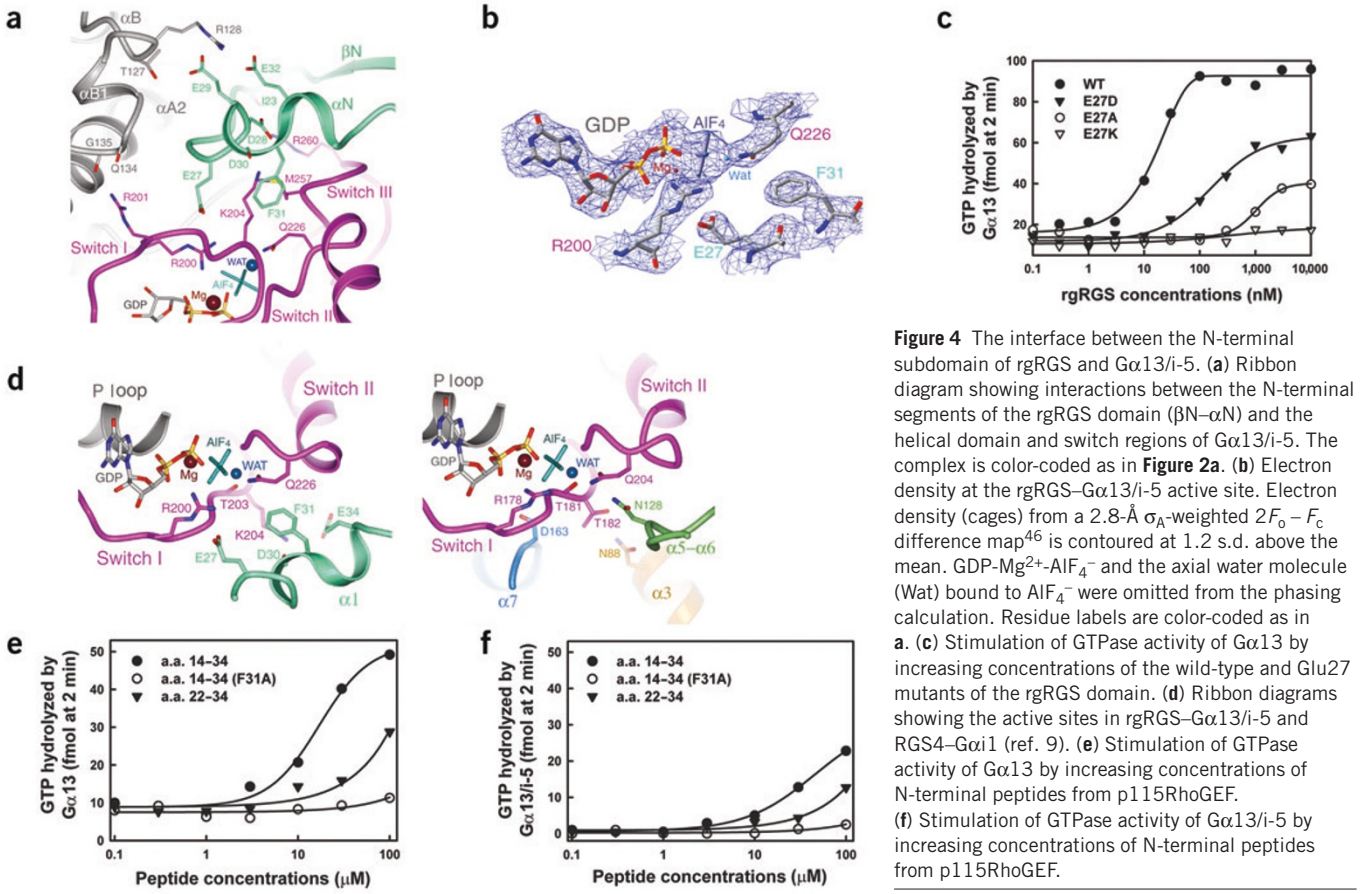

Figure 4 The interface between the N-terminal subdomain of rgRGS and Gα13/i-5. (**a**) Ribbon diagram showing interactions between the N-terminal segments of the rgRGS domain (βN–αN) and the helical domain and switch regions of Gα13/i-5. The complex is color-coded as in **Figure 2a**. (**b**) Electron density at the rgRGS–Gα13/i-5 active site. Electron density (cages) from a 2.8-Å σ_A-weighted $2F_o - F_c$ difference map[46] is contoured at 1.2 s.d. above the mean. GDP-Mg^{2+}-AlF_4^- and the axial water molecule (Wat) bound to AlF_4^- were omitted from the phasing calculation. Residue labels are color-coded as in **a**. (**c**) Stimulation of GTPase activity of Gα13 by increasing concentrations of the wild-type and Glu27 mutants of the rgRGS domain. (**d**) Ribbon diagrams showing the active sites in rgRGS–Gα13/i-5 and RGS4–Gαi1 (ref. 9). (**e**) Stimulation of GTPase activity of Gα13 by increasing concentrations of N-terminal peptides from p115RhoGEF. (**f**) Stimulation of GTPase activity of Gα13/i-5 by increasing concentrations of N-terminal peptides from p115RhoGEF.

Gαi1 in the α3–β5 and α4–β6 loops of Gα13/i-5 by their counterparts in Gα13 does not make the resulting chimera a better substrate for the GAP activity of the rgRGS domain (see **Supplementary Fig. 3** online).

DISCUSSION

Several functional inferences may be drawn from the structure of the rgRGS–Gα13/i-5 complex. First, it seems that the divergent helical and switch regions of Gα can be regarded as interchangeable functional modules that are inserted into a conserved Ras-like structural core. Thus, the functional and physical properties of one Gα isoform can be transferred even to a distantly related member of the family. Second, participation of the putative effector-binding regions of Gα13/i-5 in the complex with rgRGS is unexpected. Gα13 stimulates the RhoGEF activity that is exerted by the DH and PH domains of p115RhoGEF[2], and this stimulatory activity requires the presence of the rgRGS domain of p115RhoGEF. Hence, Gα13 may act upon the DH and PH domains of p115RhoGEF indirectly, in part through the effector-like interactions with the rgRGS domain described here. Finally, rgRGS stimulates the GTPase activity of its Gα substrates by an entirely different mechanism and through structural elements different from those used by other members of the RGS family. In this mechanism, GAP activity is mediated by the N terminus of rgRGS, and the RGS domain participates in interactions that increase the affinity of the complex. Common structural elements indicate the probable divergence of RGS domains, perhaps

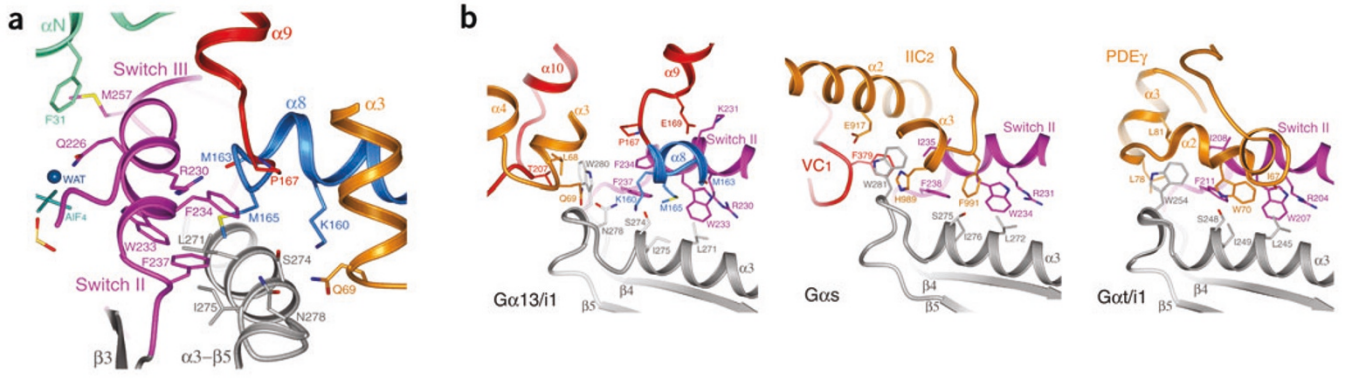

Figure 5 The interface between the RGS subdomain of rgRGS and Gα13/i-5. (**a**) Ribbon diagram showing interactions between the RGS subdomain (including the conserved RGS box) and switch II and the α3 helix of Gα13/i-5. (**b**) Ribbon diagrams showing effector-binding sites of rgRGS–Gα13/i-5, AC–Gαs[31] and PDEγ–Gαt/i1 (ref. 14). AC is gold (IIC_2) or red (VC_1), and PDEγ is gold.

Table 1 Data collection and refinement statistics

	Native
Data collection	
Space group	*C*2
Cell dimensions	
a, *b*, *c* (Å)	199.75, 105.27, 71.75
β (°)	96.91
Resolution (Å)	47–2.8
R_{sym} (%)	18.8 (58.5)
$I / \sigma I$	7.1 (1.5)
Completeness (%)	90.9 (67.4)
Redundancy	3.3
Refinement	
Resolution (Å)	2.8
Number of reflections	31,348
R_{work} / R_{free} (%)	22.9 / 29.7
Number of atoms	
Protein	8,453
Ligand or ion	68
Water	84
B-factors (Å^2)	
Protein	57.7
Ligand or ion	36.7
Water	52.9
R.m.s. deviations	
Bond lengths (Å)	0.009
Bond angles (°)	1.18

with selective binding to specific Gα subunits. However, the differences in mechanism strongly suggest that GAP function, and possibly also Gα-binding activity[32], may have arisen as a convergent function in the evolving branches of the RGS superfamily.

METHODS

Construction of Gα13/i1 expression plasmids. PCR sewing (gene splicing or overlapping PCR)[33] was used to construct cDNAs encoding chimeric Gα13/Gαi1 genes. Templates for PCR were the coding sequences of rat Gαi1 (subcloned into the pQE60 vector[34], residues 1–354) and mouse Gα13 (subcloned into the pCMV5 vector[23], residues 1–377). The sequences of primers used are available upon request. Purified PCR sewing products were cleaved with two selected restriction enzymes and inserted into expression vectors (pET28a or pET28b). Gα13/i-5, which shares the highest amino acid sequence identity with Gα13, includes amino acids 1–47 from Gαi1, 64–207 from Gα13, 185–210 from Gαi1, 234–235 from Gα13, 213–230 from Gαi1, 254–262 from Gα13 and 240–353 from Gαi1.

Expression and purification of proteins. Expression vectors encoding chimeric G-protein α subunits were transformed into *E. coli* strain JM109 (DE3) cells. Transformed cells were grown at 37 °C in LB medium in the presence of 25 mg l^{-1} kanamycin to an A_{600} of 0.5–0.6, and induced with 30 μM IPTG at 30 °C overnight. The cells were harvested by centrifugation, frozen in liquid nitrogen and lysed with addition of lysozyme, DNase I and $MgCl_2$ to final concentrations of 2 mg ml^{-1}, 1 mg ml^{-1} and 5 mM, respectively, followed by addition of Triton X-100 to a final concentration of 1% (v/v). Chimeric Gα subunits were purified to homogeneity by Ni^{2+} affinity (QIAGEN) and HiTrap Q, Superdex 200/75 chromatography (Amersham Pharmacia Biotech). Purified proteins were concentrated to 10 mg ml^{-1} in 20 mM Na^+-HEPES, pH 8.0, 5 mM β-mercaptoethanol, 100 mM NaCl and 10 μM GDP. Aliquots of 50 μl were flash-frozen with liquid nitrogen and stored at –80 °C.

The rgRGS domain (residues 1–239) of p115RhoGEF was produced in *E. coli* as a N-terminal His_6-tagged protein as described[21,35]. Gα13 was expressed in Sf9 cells and purified as described[23].

Interaction with guanine nucleotides. To assay the binding of GTPγS, Gα13/i chimeras or Gα13 (1 μM) were mixed with 5 μM [^{35}S]GTPγS and incubated at 30 °C as described[23]. At indicated time points, 10-μl aliquots were removed from the reaction mixture and assessed for protein-bound [^{35}S]GTPγS by filter binding[36].

Stimulation of GTPase activity by the rgRGS domain or an N-terminal peptide from p115RhoGEF was assessed by measuring the hydrolysis of [γ-^{32}P]GTP by Gα13/i chimeras or Gα13 as described[20].

Isothermal titration calorimetry assays. Isothermal titration calorimetry (ITC) was carried out at 6 °C (279 K) using a Microcal VP-ITC (MicroCal) calorimeter as described[37]. Protein samples were dialyzed against titration buffer (20 mM Na^+-HEPES, pH 8.0, 5 mM β-mercaptoethanol, 100 mM NaCl and 5 mM $MgCl_2$, with one of the following: 10 μM GDP, 30 μM $AlCl_3$, 10 mM NaF or 10 μM GTPγS). A typical titration of a Gα13/i chimera with the rgRGS domain of p115RhoGEF involved 25–30 injections at 3-min intervals of 8 μl of the rgRGS domain (~1 mM) into a sample cell containing 1.5 ml of the Gα13/i chimera (~110 μM).

Formation of the rgRGS–Gα13/i-5 complex. Purified Gα13/i-5 and the p115RhoGEF rgRGS domain were both treated with TEV protease to remove the N-terminal His_6-tags. The treated proteins were mixed on ice in the presence of GDP–AlF_4^-–Mg^{2+} for 15 min and concentrated to 10 mg ml^{-1} using a Centricon 10 concentrator (Millipore). The mixture was then loaded onto Superdex 200/75 tandem gel filtration columns pre-equilibrated with gel filtration buffer (20 mM Na^+-HEPES, pH 8.0, 100 mM NaCl, 5 mM β-mercaptoethanol, 10 μM GDP, 30 μM $AlCl_3$, 10 mM NaF and 5 mM $MgCl_2$). Fractions that contained rgRGS–Gα13/i-5 complex (molecular mass, ~70 kDa as judged by elution volume) were pooled and concentrated using a Centricon 30 concentrator (Millipore) to a final concentration of 10 mg ml^{-1}. Aliquots (50 μl) of the concentrated complex were flash-frozen with liquid nitrogen and stored at –80 °C.

Crystallization and data collection. The complex of Gα13/i-5 with the p115RhoGEF rgRGS domain was crystallized from 1.65–1.73 M ammonium sulfate, 100 mM Tris, pH 7.8–8.2, and 3–7% ethylene glycol by vapor diffusion at 16 °C and cryoprotected with an additional 15% (v/v) ethylene glycol. Native data were measured at 100 K at the Advanced Light Source (ALS) Beamline 8.2.1 (1° oscillation; 30 s/frame exposure time). Diffraction data were reduced using the HKL package, SCALEPACK and DENZO[38]. Crystals belong to space group *C*2 with a mosaicity of 1.6°. The relatively high R_{sym} value is largely due to the weak intensities of reflections (**Table 1**).

Structure determination and model refinement. Initial phases were generated by molecular replacement using the coordinates of Gαi1 (ref. 9) as a search model (PDB entry 1AGR, 72% amino acid sequence identity to Gα13/i-5), using AmoRe[39]. Molecular replacement using coordinates of the C-terminal segment of rgRGS (PDB entry 1IAP) did not yield convincing solutions. Model building was done using O[40]. The model was refined using CNS_SOLVE version 1.0 (ref. 41), in alternate cycles of simulated annealing, energy minimization and individual *B*-factor refinement. Putative water molecules within hydrogen-bonding distance of at least one protein atom or other water oxygen atom and with refined *B*-factors <100 Å^2 were included in the model. Weighting of crystallographic terms was chosen to minimize R_{free}. The final atomic model comprises residues 46–371 of Gα13/i-5, residues 16–37, 44–86, 93–122 and 133–233 of the p115RhoGEF rgRGS domain, GDP, AlF_4^-, Mg^{2+} and 84 water molecules. The remaining residues of Gα13/i-5 and the rgRGS domain are disordered. PROCHECK[42] indicates that >85% of the residues fall in the most favorable regions of ϕ and ψ conformational space with none in the disallowed conformations[43].

Calculations and figure rendering. Atomic representations were created using MolScript[44], POV-Ray (http://www.povray.org) and GLR (http://www.hhmi.swmed.edu/external/Doc/Gl_render/Html/gl_render.html). The electron density map was created with Swiss-PDB Viewer[45]. Structure alignments were done using O[40] (with commands LSQ_EXPLICIT and LSQ_IMPROVE).

Coordinates. The atomic coordinates and structure factors for the p115RhoGEF rgRGS domain–Gα13/i1 chimera complex have been deposited in the Protein Data Bank (accession code 1SHZ).

Note: Supplementary information is available on the Nature Structural & Molecular Biology website.

ACKNOWLEDGMENTS

We thank W. Chen, S. Gutowski, J. Hadas and A. Badejo for technical assistance, and the staff of Advanced Light Source for assistance with data collection. This work was supported by US National Institutes of Health Grants GM31954 (to P.C.S.), and DK46371 (to S.R.S.), by the Robert A. Welch foundation (to P.C.S. and S.R.S.), the Alfred and Mabel Gilman Chair in Molecular Pharmacology (P.C.S.) and the John W. and Rhonda K. Pate Professorship in Biochemistry (to S.R.S.).

COMPETING INTERESTS STATEMENT

The authors declare that they have no competing financial interests.

Received 9 August; accepted 23 November 2004
Published online at http://www.nature.com/nsmb/

1. Kozasa, T. *et al.* p115 RhoGEF, a GTPase-activating protein for Gα12 and Gα13. *Science* **280**, 2109–2111 (1998).
2. Hart, M.J. *et al.* Direct stimulation of the guanine nucleotide exchange activity of p115 RhoGEF by Gα13. *Science* **280**, 2112–2114 (1998).
3. Sah, V.P., Seasholtz, T.M., Sagi, S.A. & Brown, J.H. The role of Rho in G protein–coupled receptor signal transduction. *Annu. Rev. Pharmacol. Toxicol.* **40**, 459–489 (2000).
4. Buhl, A.M., Johnson, N.L., Dhanasekaran, N. & Johnson, G.L. Gα12 and Gα13 stimulate Rho-dependent stress fiber formation and focal adhesion assembly. *J. Biol. Chem.* **270**, 24631–24634 (1995).
5. Gohla, A., Harhammer, R. & Schultz, G. The G-protein G13 but not G12 mediates signaling from lysophosphatidic acid receptor via epidermal growth factor receptor to Rho. *J. Biol. Chem.* **273**, 4653–4659 (1998).
6. Cerione, R.A. & Zheng, Y. The Dbl family of oncogenes. *Curr. Opin. Cell Biol.* **8**, 216–222 (1996).
7. Ross, E.M. & Wilkie, T.M. GTPase-activating proteins for heterotrimeric G proteins: regulators of G protein signaling (RGS) and RGS-like proteins. *Annu. Rev. Biochem.* **69**, 795–827 (2000).
8. Zheng, B., De Vries, L. & Gist Farquhar, M. Divergence of RGS proteins: evidence for the existence of six mammalian RGS subfamilies. *Trends. Biochem. Sci.* **24**, 411–414 (1999).
9. Tesmer, J.J.G., Berman, D.M., Gilman, A.G. & Sprang, S.R. Structure of RGS4 bound to AlF_4^--activated Giα1: stabilization of the transition state for GTP hydrolysis. *Cell* **89**, 251–261 (1997).
10. Berman, D.M., Wilkie, T.M. & Gilman, A.G. GAIP and RGS4 are GTPase-activating proteins (GAPs) for the G_i subfamily of G protein α-subunits. *Cell* **86**, 445–452 (1996).
11. Druey, K.M. & Kehrl, J.H. Inhibition of regulator of G protein signaling function by two mutant RGS4 proteins. *Proc. Natl. Acad. Sci. USA* **94**, 12851–12856 (1997).
12. Srinivasa, S.P., Watson, N., Overton, M.C. & Blumer, K.J. Mechanism of RGS4, a GTPase-activating protein for G protein α-subunits. *J. Biol. Chem.* **273**, 1529–1533 (1998).
13. Posner, B.A., Mukhopadhyay, S., Tesmer, J.J., Gilman, A.G. & Ross, E.M. Modulation of the affinity and selectivity of RGS protein interaction with G α-subunits by a conserved asparagine/serine residue. *Biochemistry* **38**, 7773–7779 (1999).
14. Slep, K.C. *et al.* Structural determinants for regulation of phosphodiesterase by a G protein at 2.0 Å. *Nature* **409**, 1071–1077 (2001).
15. Fukuhara, S., Chikumi, H. & Gutkind, J.S. Leukemia-associated Rho guanine nucleotide exchange factor (LARG) links heterotrimeric G proteins of the G (12) family to Rho. *FEBS Lett.* **485**, 183–188 (2000).
16. Whitehead, I.P. *et al.* Expression cloning of *lsc*, a novel oncogene with structural similarities to the Dbl family of guanine nucleotide exchange factors. *J. Biol. Chem.* **271**, 18643–18650 (1996).
17. Fukuhara, S., Murga, C., Zohar, M., Igishi, T. & Gutkind, J.S. A novel PDZ domain containing guanine nucleotide exchange factor links heterotrimeric G proteins to Rho. *J. Biol. Chem.* **274**, 5868–5879 (1999).
18. Jackson, M. *et al.* Modulation of the neuronal glutamate transporter EAAT4 by two interacting proteins. *Nature* **410**, 89–93 (2001).
19. Wells, C.D. *et al.* Mechanisms for reversible regulation between p115 RhoGEF and GTRAP48 and the G12 class of heterotrimeric G proteins. *J. Biol. Chem.* **277**, 1174–1181 (2002).
20. Chen, Z., Singer, W.D., Wells, C.D., Sprang, S.R. & Sternweis, P.C. Mapping the Gα13 binding interface of the rgRGS domain of p115RhoGEF. *J. Biol. Chem.* **278**, 9912–9919 (2003).
21. Chen, Z., Wells, C.D., Sternweis, P.C. & Sprang, S.R. Structure of the rgRGS domain of p115RhoGEF. *Nat. Struct. Biol.* **8**, 805–809 (2001).
22. Longenecker, K.L., Lewis, M.E., Chikumi, H., Gutkind, J.S. & Derewenda, Z.S. Structure of the RGS-like domain from PDZ-RhoGEF: linking heterotrimeric G protein–coupled signaling to Rho GTPases. *Structure* **9**, 559–569 (2001).
23. Singer, W.D., Miller, R.T. & Sternweis, P.C. Purification and characterization of the α-subunit of G13. *J. Biol. Chem.* **269**, 19796–19802 (1994).
24. Wells, C.D., Gutowski, S., Bollag, G. & Sternweis, P.C. Identification of potential mechanisms for regulation of p115 RhoGEF through analysis of endogenous and mutant forms of the exchange factor. *J. Biol. Chem.* **276**, 28897–28905 (2001).
25. Berlot, C.H. & Bourne, H.R. Identification of effector-activating residues of Gs α. *Cell* **68**, 911–922 (1992).
26. Skiba, N.P., Bae, H. & Hamm, H.E. Mapping of effector binding sites of transducin α-subunit using Gαt/Gαi1 chimeras. *J. Biol. Chem.* **271**, 413–424 (1996).
27. Eisenhaure, T.M., Francis, S.A., Willison, L.D., Coughlin, S.R. & Lerner, D.J. The Rho guanine nucleotide exchange factor Lsc homo-oligomerizes and is negatively regulated through domains in its carboxyl terminus that are absent in novel splenic isoforms. *J. Biol. Chem.* **278**, 30975–30984 (2003).
28. Chikumi, H. *et al.* Homo- and hetero-oligomerization of PDZ-RhoGEF, LARG and p115RhoGEF by their C-terminal region regulates their *in vivo* Rho GEF activity and transforming potential. *Oncogene* **23**, 233–240 (2004).
29. Coleman, D.E. *et al.* Structures of active conformations of Giα1 and the mechanism of GTP hydrolysis. *Science* **265**, 1405–1412 (1994).
30. Sondek, J., Lambright, D.G., Noel, J.P., Hamm, H.E. & Sigler, P.B. GTPase mechanism of G proteins from the 1.7 Å crystal structure of transducin α-GDP-AlF_4^-. *Nature* **372**, 276–279 (1994).
31. Tesmer, J.J., Sunahara, R.K., Gilman, A.G. & Sprang, S.R. Crystal structure of the catalytic domains of adenylyl cyclase in a complex with Gsα.GTPγS. *Science* **278**, 1907–1916 (1997).
32. Sterne-Marr, R. *et al.* G protein–coupled receptor kinase 2/Gαq/11 interaction. A novel surface on a regulator of G protein signaling homology domain for binding Gα subunits. *J. Biol. Chem.* **278**, 6050–6058 (2003).
33. Horton, R.M., Hunt, H.D., Ho, S.N., Pullen, J.K. & Pease, L.R. Engineering hybrid genes without the use of restriction enzymes: gene splicing by overlap extension. *Gene* **77**, 61–68 (1989).
34. Lee, E., Linder, M.E. & Gilman, A.G. Expression of G protein α-subunits in *Escherichia coli*. *Methods Enzymol.* **237**, 146–164 (1994).
35. Wells, C., Jiang, X., Gutowski, S. & Sternweis, P.C. Functional characterization of p115 RhoGEF. *Methods Enzymol.* **345**, 371–382 (2002).
36. Northup, J.K., Smigel, M.D. & Gilman, A.G. The guanine nucleotide activating site of the regulatory component of adenylate cyclase. Identification by ligand binding. *J. Biol. Chem.* **257**, 11416–11423 (1982).
37. Adhikari, A. & Sprang, S.R. Thermodynamic characterization of the binding of activator of G protein signaling 3 (AGS3) and peptides derived from AGS3 with Gαi1. *J. Biol. Chem.* **278**, 51825–51832 (2003).
38. Otwinowski, Z. & Minor, W. Processing of X-ray diffraction data collected in oscillation mode. *Methods Enzymol.* **276**, 307–326 (1997).
39. Navaza, J. AMoRe: an automated package for molecular replacement. *Acta Crystallogr. A* **50**, 157–163 (1994).
40. Jones, T.A., Zou, J.Y., Cowan, S.W. & Kjeldgaard, M. Improved methods for building protein models in electron density maps and the location of errors in these models. *Acta Crystallogr. A* **47**, 110–119 (1991).
41. Brunger, A.T. *et al.* Crystallography & NMR system: a new software suite for macromolecular structure determination. *Acta Crystallogr. D* **54**, 905–921 (1998).
42. Laskowski, R.A., MacArthur, M.W., Moss, D.S. & Thornton, J.M. PROCHECK: a program to check the stereochemical quality of protein structures. *J. Appl. Crystallogr.* **26**, 283–291 (1993).
43. Ramachandran, G.N. & Sassiekharan, V. Conformation of polypeptides and proteins. *Adv. Protein Chem.* **28**, 283–437 (1968).
44. Kraulis, P.J. MOLSCRIPT: a program to produce both detailed and schematic plots of protein structures. *J. Appl. Crystallogr.* **24**, 946–950 (1991).
45. Guex, N. & Peitsch, M.C. SWISS-MODEL and the Swiss-PdbViewer: an environment for comparative protein modeling. *Electrophoresis* **18**, 2714–2723 (1997).
46. Read, R.J. Improved Fourier coefficients for maps using phases from partial structures with errors. *Acta Crystallogr. A* **42**, 140–149 (1986).